Materials Science Forum
ISSN: 1662-9752, Vol. 1191, pp 37-42
doi:10.4028/p-lyf5Sy
© 2026 The Author(s). Published by Trans Tech Publications Ltd, Switzerland.
Submitted: 2025-09-29
Revised: 2025-12-24
Accepted: 2026-02-23
Online: 2026-05-19

Characterization of the Electric Field in Silicon Carbide Detectors by Optical Beam Induced Current

S. De Luca[1,a*], A. S. Mancuso[1,2,b], A. Muoio[1,c], E. Sangregorio[1,d] and F. La Via[1,e]

[1]CNR-IMM, sede di Catania Strada VIII 5 - Zona Industriale I-95121 Catania, Italy

[2]Università degli Studi di Catania, Via S. Sofia n. 64, 95123 Catania, Italy

[a]saverio.deluca@cnr.it, [b]alfio.mancuso@phd.unict.it, [c]annamaria.muoio@cnr.it, [d]Enrico.Sangregorio@imm.cnr.it, [e]francesco.lavia@cnr.it

Keywords: 4H-SiC detectors, OBIC (Optical Beam Induced Current) technique, electric field characterization, Synopsis TCAD simulations.

Abstract. Silicon carbide (SiC) is a wide-bandgap semiconductor that has attracted considerable attention for the development of advanced electronic and sensing devices. Thanks to its combination of high breakdown field, excellent thermal conductivity, and chemical stability, SiC enables operation in conditions where conventional semiconductors fail. In this study, the Optical Beam Induced Current (OBIC) technique will be employed to analyze the electric field distribution within the structure of SiC bipolar diodes featuring varying epitaxial layer thicknesses. To create OBIC signal we have used ultraviolet laser beam. We have tested bipolar diodes with both 10 µm and 100 µm epilayer thicknesses. We have obtained several OBIC signals by re-scanning the same location at different reverse voltages applied to the same SiC diode. Also, Synopsis TCAD simulations of the electric field are reported for both diodes. In these simulations it is possible to observe the increase of the electric field at the edge of the devices that are observed by the OBIC measurements. In conclusion, OBIC technique aids in optimizing device design and improving overall performance.

Introduction

Silicon carbide (SiC) is a wide-bandgap semiconductor known for its outstanding characteristics, making it especially suitable for high-voltage and harsh-environment applications [1–3]. Compared to conventional silicon (Si)-based power devices, SiC consistently demonstrates superior performance [4]. For this reason, 4H-SiC–based devices are increasingly considered as a promising solution to meet the rising demand for high blocking voltages, with requirements ranging from about 3 kV for train electronics to more than 10 kV for electrical distribution networks. In this context, a new generation of 4H-SiC power devices has been developed at CNR-IMM in collaboration with ASM company, aiming to meet the needs of next-generation high-voltage applications. The new-designed devices were tested using the Optical Beam Induced Current (OBIC) technique, a characterization technique that relies on the current generated by an ultraviolet laser (325 nm) to study the electric field in the device at different voltages. The results were compared to numerical simulations performed using the Synopsys Sentaurus TCAD simulation toolkit [5].

Tested Devices

The devices investigated in this work are 4H-SiC bipolar diodes developed by CNR-IMM with the support of ASM company. Two types of diodes were fabricated, primarily differing in the thickness and doping concentration of the epitaxial layer to optimize their performance for different blocking voltage ranges. The device designed to operate at 3 kV was grown on n-type 4H-SiC substrates with an epitaxial layer of 10 µm thickness and a doping concentration of 10^{15} cm^{-3}, while the device designed to operate at 10 kV was fabricated on the same substrate material but featured a thicker

This article is an open access article under the terms and conditions of the Creative Commons Attribution (CC BY) license (https://creativecommons.org/licenses/by/4.0)

epitaxial layer of 10 µm with a lower doping concentration of 10^{14} cm^{-3}. In both cases, the P^+/N junction was established by epitaxially grown a P^+ layer on top of the N^- epitaxial layer, with a doping concentration of 10^{18} cm^{-3}. A large active area of 2,25 cm^2 was designed for both devices, allowing them to sustain currents on the order of several amperes. To ensure stable operation at high voltages, special edge termination structures were implemented to shape the electric field at the device periphery, preventing premature breakdown. Specifically, a P^- Junction Termination Extension (JTE) and a N^+ Field Stop guard ring was realized through ion implantation to close the field lines and so confine the electric field inside the active area of detectors. The design of the devices, including the active region and the edge termination, is illustrated in Fig. 1, which shows a schematic lateral cross-section of the 4H-SiC bipolar diodes.

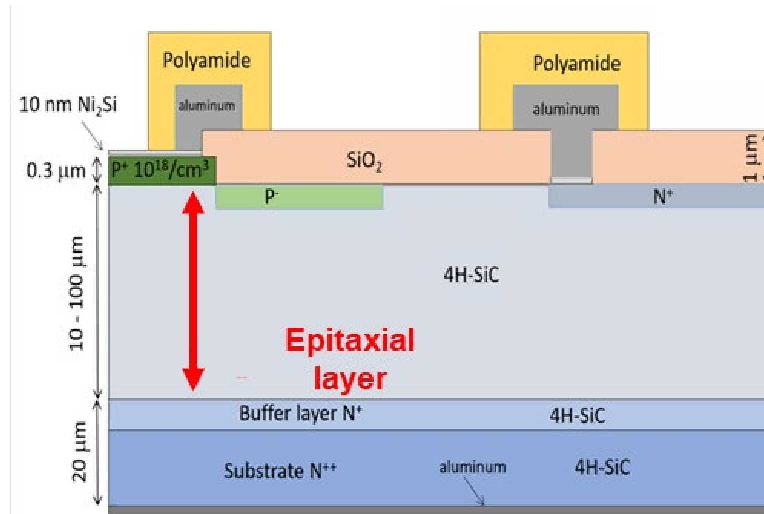

Fig. 1. Lateral cross-section of the 4H-SiC diode, illustrating the active region (on the left) and the edge termination structure (on the right), including the P^- JTE and the N^+ Field Stop Guard Ring.

Experimental Setup and OBIC Technique

To create electron-hole pairs inside the semiconductor, a 325 nm UV laser beam was used, as shown in Fig. 2 (a), where the structure of the used bipolar diode with a Junction Termination Extension (JTE) has been reported. The laser beam has been focused by 10x and 40x objectives, and the resulting spot diameters size were of the order of 10 – 5 mm respectively. The focused laser beam was moved on the surface of the device with steps of 2 microns. Both 10 and 100 µm bipolar diodes were tested under revers bias conditions, with voltages in the range of 10 – 200 V. The voltage was provided and measured by a Keithley 2450 and 2470 SMU (Source Measurement Unit). The OBIC signals were then mapped in 2-directions (X and Y) or along one line using a dedicated LabSpec6 software. Fig. 2 (b) shows the OBIC signal generated during a linear laser scan of the device. Four distinct regions can be identified, arising from the different interactions between the laser and the various layers of the material.

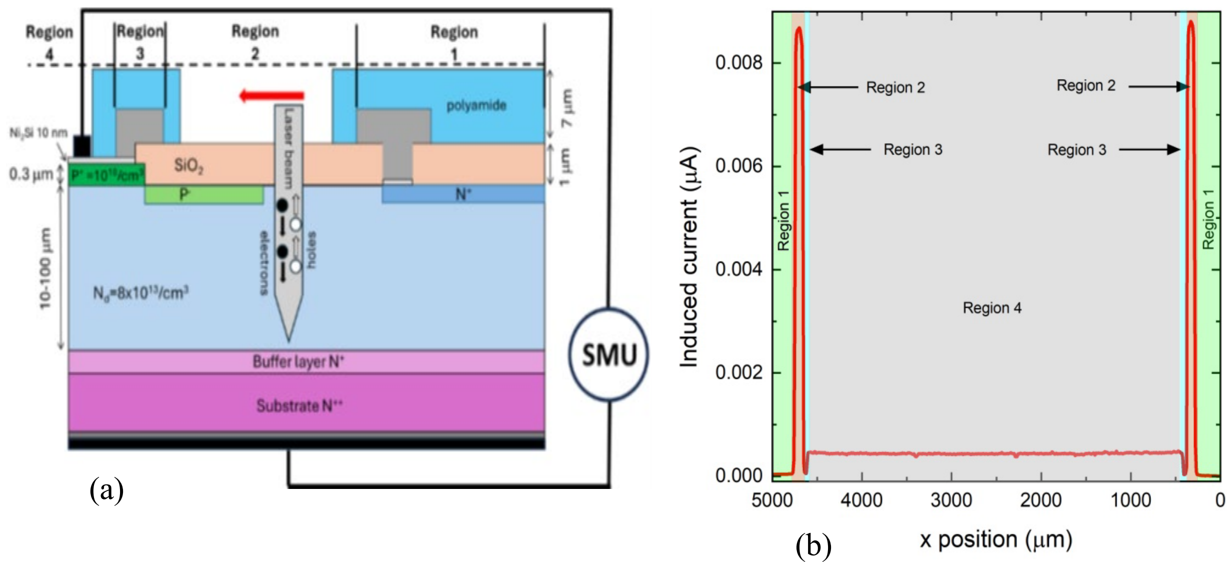

Fig. 2. (a) Schematic representation of experimental set-up and UV laser used to generate carriers (electron-hole pairs). (b) OBIC signal obtained along a straight line of the entire device.

Results and Discussions

The intensity of the photo-generated current is linked to the intensity of the average electric field and therefore to the reverse voltage applied to the detector under test. In Fig. 3. (a) the four different regions can be better observed. Until 50 µm the OBIC is about zero because the laser is outside the active region of the device (Region 1), this signal represents the background current of the detector. Starting from 50 µm an increase of the OBIC signal is observed, as the laser is irradiating the edge structure of the device (Region 2). Close to 200 µm a large decrease of the current is observed as the laser beam reaches the Al metallization layer (Region 3). Then, starting from about 230 µm, a large flat region is visible in correspondence of the anode of the device (Region 4). In this case, the intensity of OBIC is lower with respect to the edge of the device (Region 2) because the thin silicide layer on the top of the P^+ epitaxial layer produces a reduction of the laser intensity that arrives in the depleted layer, due to its high reflectivity. The same behavior has been observed on the other side of the detector, as shown in Fig. 2 (b).

OBIC signals were acquired at different reverse biases (up to 200 V) by re-scanning the same location with the laser. The increased electric field caused by an increase in reverse voltage results in an increase of the OBIC signal at the same location, as observed in Region 2 of Fig. 3 (a). Here, using a 10 V reverse bias, the induced current obtained by the laser scan decreases towards the edge of the device (going throws Region 1). This result is linked to a low electric field induced by the reverse polarization. As the reverse bias increases to 50 V, a box-like OBIC signal suggests a uniform electric field in this region. By increasing even more the reverse bias, a small peak of the OBIC current is observed close to the edge of Region 2, suggesting a higher value of the field in this region. The same behavior is observed in the thicker diode (Fig. 3. b), where the OBIC peak is visible already at 50 V. By the amplitude of the OBIC signal in Region 2, the lateral depletion width was calculated at different tensions, the results are reported in Fig. 4 (b).

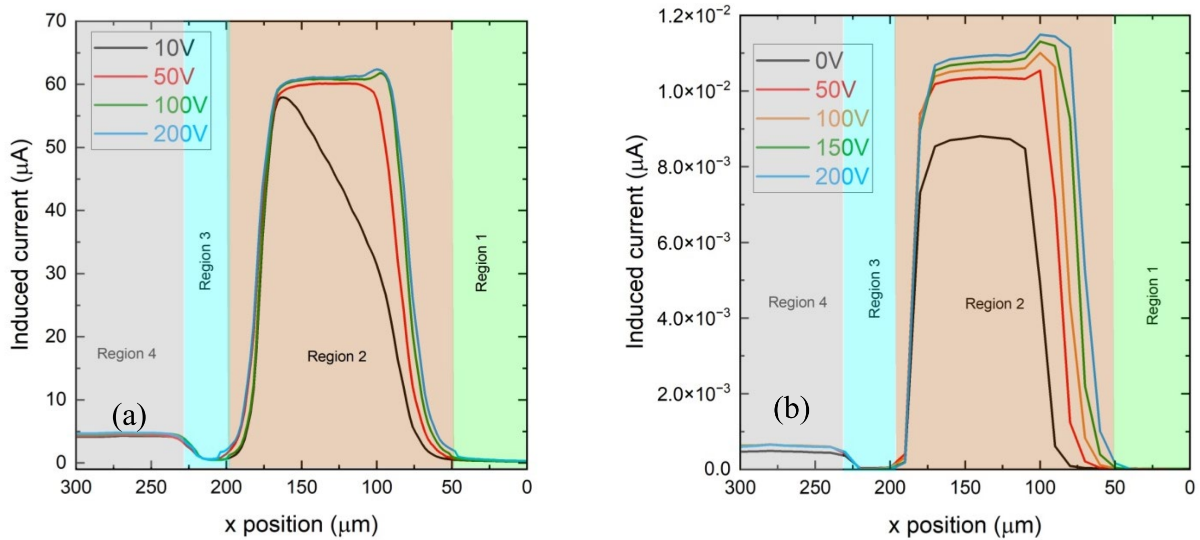

Fig. 3. (a) Photo-current produced by UV laser in 10 μm (a) and 100 μm (b) epilayer thickness SiC detectors along the four regions close to the device edge at different reverse biases. The different amplitude of induced currents depends on the different filters used for the two detectors.

o connect experimental data with the structures of the new detectors, several simulations were carried out using Synopsys Sentaurus TCAD for both 10 and 100 μm epitaxial layer devices. Fig. 4 (a) shows the electric field distribution of the 100 μm epitaxial layer device at 500 V. Under these conditions, the simulation reveals a high-intensity electric field point (marked by a red circle) at the boundary between Region 2 and Region 1, responsible for the induced current peak observed experimentally.

Fig. 4 (b) compares the experimental and simulated lateral depletion widths of the boundary region for both devices as a function of the square root of the applied reverse bias. In both cases, experimental and simulated data follow a linear trend up to ~170 μm, where saturation of the lateral depletion occurs. The simulated depletion width of the 10 μm device shows a better agreement with the corresponding experimental data compared to the 100 μm device. This discrepancy may be related to the different objectives used during the characterization of the two devices.

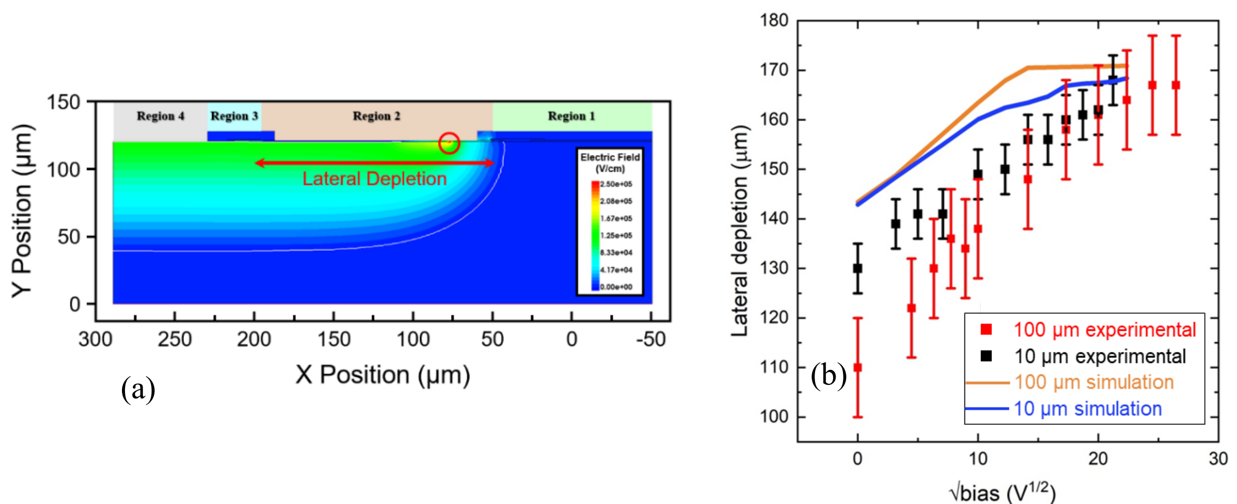

Fig. 4. (a) Simulated electric field distribution of the 100 μm epitaxial layer device at 500V, showing the peak close to the edge of Region 2 (red circle) and the lateral depletion region. (b) Comparison between simulated and experimental lateral depletion widths for the 10 μm and 100 μm epitaxial layers devices as a function of the square root of the applied reverse bias.

Finally, to highlight the correlation between the OBIC signal and the electric field within the device, the mean electric field and the induced current at different reverse bias were evaluated at specific x positions. Fig.5 reports the simulated mean electric field (averaged along the y direction) and the corresponding experimental induced current measured at different reverse biases for the 100 µm epitaxial layer device at x = 150 µm. The electric field was averaged over the first 20 µm from the surface, corresponding to the laser interaction volume. As the reverse bias increases, the induced current rises, reflecting the increase in the mean electric field, which enhances carrier drift velocity and reduces recombination losses. Once a 100% charge collection efficiency (CCE) is reached, further increases in the applied bias, and thus in the internal electric field, do not result in a higher induced current, since all generated carriers are already collected. This behavior explains the exponential correlation observed in Fig. 5.

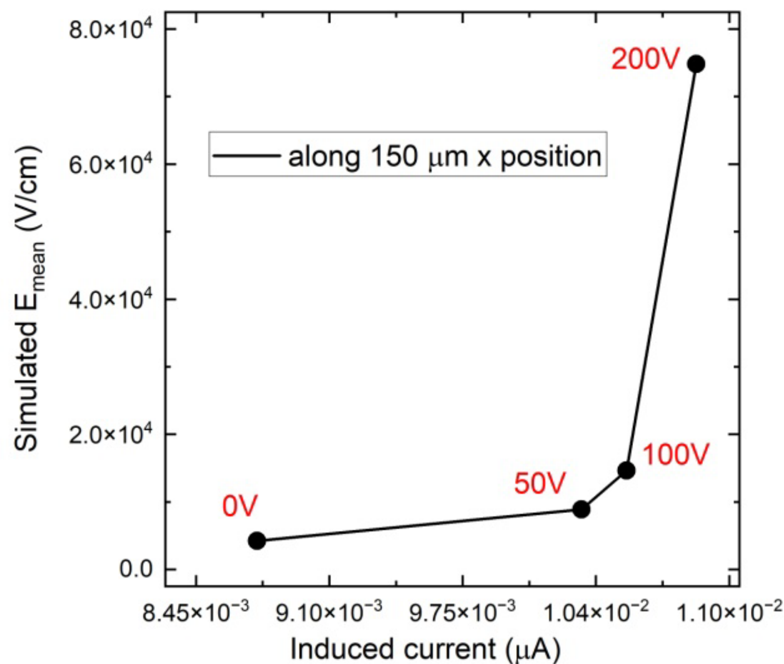

Fig. 5. Simulated mean electric field vs induced current obtained in the plateau area in Region 2 (position x = 150 µm) at different reverse bias for 100 µm epitaxial layer device. The electric field was averaged along y line for the first 20 microns of depth from the surface. This is the penetration thickness of the used UV-laser.

Conclusions

Several measurements and simulations were performed on a new generation of 4H-SiC devices. The electric field distribution within SiC bipolar diodes under reverse bias was characterized using the Optical Beam Induced Current (OBIC) technique with a spatial resolution of 5 – 10 µm. This approach enabled the investigation of the edge structure of high-voltage P^+/N diodes through the analysis of OBIC signals. The experimental results were compared with TCAD simulations, and optimization of the simulation parameters is in progress to reduce the mismatch with the experimental data at low bias for both devices. Future work will focus on the characterization of the 100 µm epitaxial layer device using a 349 nm UV laser, in order to gain deeper insight into the electric field distribution within the thick epitaxial region.

References

[1] K. Shenai et al., IEEE Trans. Electron. Dev. 36 (9) (1989) 1811–1823.

[2] C. Raynaud et al., Diam. Relat. Mater. 19 (2010) 1–6.

[3] T. Mizushima et al., Proc. Int. Symp. Power Semicond. Dev. IC's (2014) 277–280, 10.10.1109/ ISPSD.2014.6856030. WBGS Young, ICSCRM Michael, J. Appl. Phys. 00, 5050 (2021).

[4] S. Tudisco et al., Sensors 18.7 (2018): 2289.

[5] Synopsys Sentaurus TCAD Ver. J-2014.09, Synopsys, Inc., Mountain View, CA, USA. (2014). Available online: https://www.synopsys.com/home.aspx.